MOLECULAR AND CELLULAR BIOLOGY, Mar. 2006, p. 1879–1887 Vol. 26, No. 5
0270-7306/06/$08.00+0 doi:10.1128/MCB.26.5.1879–1887.2006


# Mice Lacking the Nuclear Pore Complex Protein ALADIN Show Female Infertility but Fail To Develop a Phenotype Resembling Human Triple A Syndrome

Angela Huebner,[1]* Philipp Mann,[1] Elvira Rohde,[2] Angela M. Kaindl,[1,3] Martin Witt,[4] Paul Verkade,[5] Sibylle Jakubiczka,[6] Mario Menschikowski,[7] Gisela Stoltenburg-Didinger,[8] and Katrin Koehler[1]

*Children's Hospital, Technical University Dresden, Dresden, Germany[1]; Department of Molecular Genetics, Institute of Molecular Pharmacology, Berlin, Germany[2]; Department of Neuropediatrics, Charité, University Medical School, Berlin, Germany[3]; Department of Anatomy, Technical University Dresden, Dresden, Germany[4]; Max Planck Institute of Molecular Cell Biology and Genetics, Dresden, Germany[5]; Institute of Human Genetics, Otto-von-Guericke University, Magdeburg, Germany[6]; Institute of Clinical Chemistry and Laboratory Medicine, Technical University Dresden, Dresden, Germany[7]; and Institute of Neuropathology, Charité, University Medical School, Berlin, Germany[8]*

Received 9 November 2005/Accepted 6 December 2005

**Triple A syndrome is a human autosomal recessive disorder characterized by adrenal insufficiency, achalasia, alacrima, and neurological abnormalities affecting the central, peripheral, and autonomic nervous systems. In humans, this disease is caused by mutations in the *AAAS* gene, which encodes ALADIN, a protein that belongs to the family of WD-repeat proteins and localizes to nuclear pore complexes. To analyze the function of the gene in the context of the whole organism and in an attempt to obtain an animal model for human triple A syndrome, we generated mice lacking a functional *Aaas* gene. The *Aaas*$^{-/-}$ animals were found to be externally indistinguishable from their wild-type littermates, although their body weight was on the average lower than that of wild-type mice. Histological analysis of various tissues failed to reveal any differences between *Aaas*$^{-/-}$ and wild-type mice. *Aaas*$^{-/-}$ mice exhibit unexpectedly mild abnormal behavior and only minor neurological deficits. Our data show that the lack of ALADIN in mice does not lead to a triple A syndrome-like disease. Thus, in mice either the function of ALADIN differs from that in humans, its loss can be readily compensated for, or additional factors, such as environmental conditions or genetic modifiers, contribute to the disease.**

The triple A syndrome (also known as Allgrove syndrome; MIM #231550) is a rare human autosomal recessive disorder characterized by the clinical triad of achalasia of the cardia (increased tone of the lower esophagus sphincter with consecutive dilation of the esophagus), alacrima (deficiency of tear production), and adrenocorticotropic hormone (ACTH)-resistant adrenal insufficiency (1). In addition to the three main symptoms, patients suffer from a variety of progressive neurological symptoms that indicate an involvement of the central, peripheral, and autonomic nervous systems. A development of mental retardation, mixed motor-sensory neuropathy, and severe dysautonomia can lead to disability and considerable impairment in quality of life (3). The involvement of other organ systems demonstrated by palmoplantar hyperkeratosis, scoliosis, osteoporosis, caries, and parodontosis, as well as short stature, point to the multisystemic character of the disorder (3, 11, 16). The disease was linked to chromosome 12q13 (8, 12, 19, 25), and the causative gene, *AAAS*, was identified. *AAAS* encodes a 546-amino-acid protein designated ALADIN (for "alacrima-achalasia-adrenal insufficiency neurologic disorder") (9, 20). ALADIN belongs to the WD-repeat protein family and localizes to nuclear pore complexes (NPCs), which are the sole site of nucleocytoplasmic transport (5, 6).

Here, we report the generation of transgenic mice which carry a targeted disruption of the *Aaas* gene. Mice deficient in ALADIN unexpectedly exhibit only mildly abnormal behavior and minor neurological defects.

## MATERIALS AND METHODS

**Experimental animals.** All mice were housed in the animal care facility (Experimental Center) of the Technical University Dresden, Dresden, Germany. All procedures were approved by the Regional Board for Veterinarian Affairs (AZ 24-9168.21-1-2002-1) in accordance with the institutional guidelines for the care and use of laboratory animals. Animals were group housed except during actual experimental procedures, when single housing was required. Mice were kept under specific-pathogen-free conditions at a constant temperature (22 ± 1°C) and a constant light/dark cycle at all times (12:12 with lights on at 0530 h). Mice were weaned onto ssniff R/M-H (ssniff GmbH, Soest, Germany) (19% protein, 4.9% fibers, 3.3% fat, 12.2 MJ/kg). C57BL/6J and 129/Ola mice were obtained from Harlan-Winkelmann GmbH, Borchen, Germany.

**Generation of *Aaas*-deficient (*Aaas*$^{-/-}$) mice.** The murine *Aaas* locus was amplified from genomic DNA of 129/Ola embryonic stem (ES) cells with Platinum *Pfx* DNA Polymerase (Invitrogen GmbH, Karlsruhe, Germany). The *Aaas* targeting vector was constructed based on the pPNT vector (21). The plasmid was opened by BamHI/KpnI digestion, and a 1.5-kb 5′ homologous genomic fragment corresponding to the region adjacent to the start codon of the *Aaas* gene was inserted by sticky end cloning. In a second step, as 3′ homology a 3.3-kb fragment encompassing the genomic region from intron 2 to exon 6 of the *Aaas* gene was inserted in the XhoI/NotI site of pPNT.

After linearization with NotI, 25 μg of the targeting vector was electroporated into E14.1 (subclone KPA) ES cells derived from 129/Ola mice (15). The clones

* Corresponding author. Mailing address: Children's Hospital, Technical University Dresden, Fetscherstrasse 74, 01307 Dresden, Germany. Phone: 49-351-458-2926. Fax: 49-351-458-4334. E-mail: angela.huebner@mailbox.tu-dresden.de.

were grown under double selection (280 μg/ml G418, 2 μM ganciclovir), and genomic DNA from doubly resistant colonies was tested for homologous recombination events by PCR using primers located upstream of the 5′ homologous region (P1: 5′-AAGCCCCTTATACTCCCTGT-3′) and in the PGK-neo cassette (P2: 5′-CATCGCCTTCTATCGCCTTCT-3′). PCR results were confirmed by Southern hybridization. Chimeras were generated by standard techniques from two independent clones with the desired mutation. Upon germ line transmission, animals carrying the mutant *Aaas* allele were intercrossed. Genotypes were determined by multiplex PCR using the following primers: for the wild-type allele, reverse primer P3 (5′-TAGAGAAGACCTGATGGACGGCA-3′); for the knockout allele, reverse primer P4 (5′-GCTGACCGCTTCCTCGTGCTT TAC-3′) in combination with forward primer P5 (5′-TCGTTTGTCCTGTAC GGCTACCC-3′) for both alleles. Mice used for analysis were of a 129/Ola-C57BL/6 mixed background.

**DNA and RNA analysis.** For Southern hybridization, genomic DNA of ES cells was extracted with phenol-chloroform and precipitated with ethanol. Genomic DNA from tail biopsies was prepared with the DNeasy Tissue Kit (QIAGEN, Hilden, Germany) according to the manufacturer's instructions. After restriction enzyme digestion with BglI, genomic DNA was separated by agarose gel electrophoresis on 0.7% agarose gels in 1× Tris-acetate-EDTA buffer for 20 h at 1.2 V/cm. DNA was then transferred to Hybond N+ (Amersham Biosciences, Freiburg, Germany) and hybridized with the radioactively labeled probe by standard techniques. Bands were visualized by autoradiography.

Northern blot analysis was performed using standard radioactive techniques with total RNA isolated by TRIzol reagent (Invitrogen GmbH, Karlsruhe, Germany). Fifteen micrograms of total testes RNA from wild-type, heterozygous, and mutant mice were separated on an agarose gel, blotted, and hybridized with an *Aaas* cDNA probe binding to exons 1 and 2. After stripping, the filter was reprobed with β-actin cDNA and full-length mouse cDNA of other WD-repeat proteins from the NPC (Nup37, Nup43, Sec13L, RAE1). The 5′ cDNA ends were synthesized by 5′ rapid amplification of cDNA ends (5′ RACE) using the SMART RACE cDNA Amplification Kit (Clontech, Palo Alto, CA) according to the instruction manual, followed by automated sequencing using the BigDye Terminator Cycle Sequencing Kit and ABI 3100 (Applied Biosystems, Foster City, CA).

**Generation of anti-ALADIN polyclonal antibody.** Anti-peptide antibody was generated against a 17-amino-acid C-terminal region of ALADIN (Ser382 to Glu398). Synthetic peptide-containing terminal cysteine residues were conjugated to keyhole limpet hemocyanin. The peptide constructs were used to immunize rabbits. Peptide synthesis and immunization were done by Pineda-Antikörper-Service, Germany. Anti-peptide immunoglobulin G antibody was purified from sera using protein A Sepharose and dialyzed against phosphate-buffered saline.

**Western blotting.** Tissues used for Western blots were dissected from wild-type and knockout mice and were homogenized in ice-cold lysis buffer (50 mM Tris-HCl [pH 7.4], 150 mM NaCl, 1% Triton X-100, 0.3% Empigen BB, 1× protease inhibitor cocktail with EDTA). After 10 min of centrifugation at 1,000 × *g*, 3 volumes of supernatant (100 μg protein) were mixed with 1 volume of 4× reducing sodium dodecyl sulfate (SDS) sample buffer (Roti-Load 1; Carl Roth GmbH, Karlsruhe, Germany) and loaded onto a 10% SDS-polyacrylamide gel. The gel was blotted onto nitrocellulose using a semidry blotting technique. Nonspecific binding of proteins to the membrane was blocked by incubation in phosphate-buffered saline containing 5% skim milk and 0.1% Tween 20. The membrane was then probed with rabbit anti-ALADIN polyclonal antibody (1: 2,000) followed by peroxidase-labeled anti-rabbit antibody and enhanced chemiluminescence detection (Amersham Biosciences, Freiburg, Germany). After stripping, the membrane was reprobed with an anti-β-actin monoclonal antibody at 1:10,000 (Sigma-Aldrich, Seelze, Germany).

**Histological analysis.** Two pairs of male and female wild-type and *Aaas*$^{-/-}$ mice were sacrificed to obtain different organs for tissue sections. Tissue samples were fixed in 4% formaldehyde and embedded in paraffin. Paraffin sections (4 μm) were stained with hematoxylin-eosin, Goldner trichrome, or 0.2% *p*-phenylenediamine (Sigma-Aldrich, Seelze, Germany) and analyzed for histological abnormalities.

**Electron microscopy.** Mice were anesthetized and subsequently perfusion fixed through the heart with 2% glutaraldehyde in phosphate buffer according to standard protocols. Selected tissues were dissected, and small pieces were processed for standard Epon embedding. Mouse embryonic fibroblasts were grown on sapphire disks and high-pressure frozen with an EM PACT2 + RTS High Pressure Freezer (Leica Microsystems, Wetzlar, Germany). The frozen samples were freeze substituted in 1% osmiumtetraoxide and 0.1% uranylacetate in acetone and subsequently embedded in Epon. Ultrathin sections were analyzed in an electron microscope.

**Hormone measurements.** The concentration of adrenocorticotropic hormone in plasma was measured with a sequential immunometric assay kit obtained from DPC Biermanm GmbH (Bad Nauheim, Germany). Corticosterone concentrations were measured with a double-antibody $^{125}$I radioimmunoassay kit from ICN Biomedicals GmbH (Eschwege, Germany) according to the manufacturer's instructions.

**Behavioral and motor function phenotyping.** Behavioral and motor function analyses were conducted with 154 animals aged 10 ($n$ = 40), 20 ($n$ = 35), and 30 weeks ($n$ = 79). The tests were performed on three consecutive days between 0800 and 1300 h. The order of testing has been designated from least invasive to most invasive (17). Body weight was measured weekly.

**(i) Common behavior.** The behavior of mice was analyzed according to a standard test battery originally reported by Irwin (14). Home cage activity was monitored in a viewing jar (body position, spontaneous activity, defecation, urination) and in an arena (transfer arousal, tail elevation, gait). For evaluation of simple neurological reflexes, the eye blink reflex, ear twitch reflex, visual placing reflex, whisker-orienting reflex, acoustic startle reflexes, and plantar snatch reflex were tested.

**(ii) Open field activity.** Locomotor activity was evaluated by placing mice in an open field arena. Each mouse was monitored for 10 min in a test chamber of 46 by 46 by 50 cm (TSE, Bad Homburg, Germany) by light beam interruptions measuring animal position per 250 ms to assess horizontal and vertical locomotion. Total distance (locomotor activity) and vertical activity (rearing), measured by number of photobeam interruptions, were recorded.

**(iii) Light-dark exploration test.** The light-dark exploration test measures the conflict between the natural tendency of mice to explore a novel environment and their tendency to avoid a brightly lit, anxiety-provoking open area. It was conducted as previously described (4, 10). The apparatus consisted of a polypropylene cage (54 by 32 by 21 cm) separated into two compartments by a partition, which had a small opening (3.5 by 5 cm) at ground level. The larger compartment (36 cm long) was open at the top, transparent, and brightly illuminated by a special lamp (approximately 4,000 lx). The smaller compartment (18 cm long) was closed at the top and painted black. Within an observation time of 6 min the number of light-dark transitions between the two compartments and the total time spent in each compartment were recorded.

**(iv) Rotarod test.** Motor coordination and balance were tested using an accelerating Rotarod test (TSE Systems, Mannheim, Germany). The Rotarod test was performed by placing a mouse on a motor-driven rotating drum flanked by two larger plates and measuring the time each animal was able to maintain its balance walking on top of the rod. The speed of the Rotarod accelerated from 4 to 40 rpm over a 5-min period. Mice were customized to the procedure by two trials of 60 s each walking on the rod on two consecutive days. The third trial, considered the test trial, was performed on the second day at 2 h after the second trial (24). The mice were returned to their home cage during each intertrial rest interval.

**(v) Climbing activity test.** After a habituation time of 30 min in climbing cages made of screen wire (20 cm in height and 12 cm in diameter), the spontaneous climbing activity of mice was scored for 5 min as previously described (18). Five times at the beginning of succeeding minutes the behavior of mice was measured as follows: all paws on the floor, 0 points; forepaws on the wall, 1 point; forepaws and one hind paw on the wall, 1.5 points; all paws on the wall, 2 points. After 5 min, points were added to obtain a final sum.

**(vi) Wire hang test.** In the wire hang test, the ability to hang upside-down from a wire screen was tested using a cage grid. A square area of the screen was taped off in order to confine mice to a 30- by 30-cm section of the screen. The screen was divided into nine sections. After mice were placed on the screen, the screen was waved gently in the air three times to force the mice to grip the wires. The screen was then immediately turned upside down above a large rodent housing cage. Latency to falling into the tub cage and the change of quadrants was recorded. Mice that fell in less than 10 s were given a second trial. Mice that did not fall during the 10-min trial period were removed and given the maximum score. The number of changes of quadrants indicated explorative behavior.

**Statistical analysis.** Statistical analysis of behavioral data was carried out with SPSS 11.5 using the Mann-Whitney U test for nonparametric independent two-group comparison. Differences were considered significant when $P$ values were $<0.05$.

## RESULTS

**Generation of *Aaas* knockout mice.** The *Aaas* gene was inactivated by integration of a neomycin resistance cassette (PGK-neo), replacing the start codon via homologous recom-

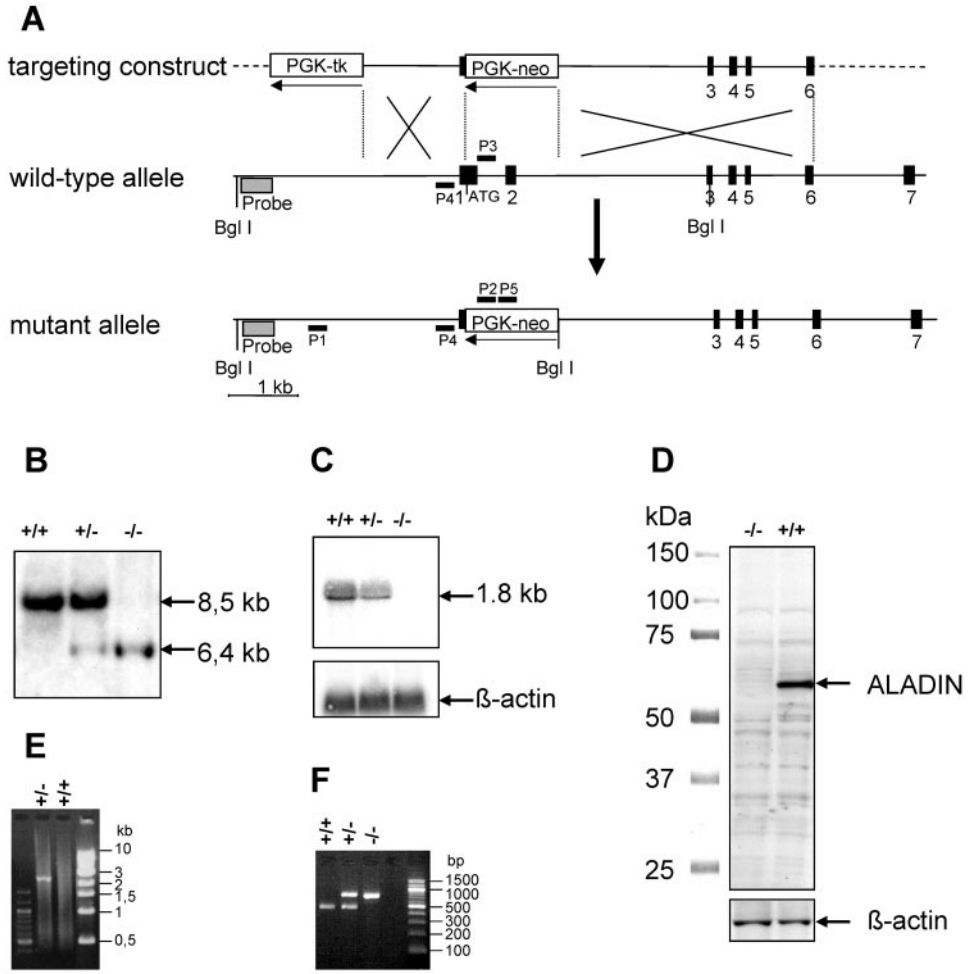


FIG. 1. Generation of a mouse strain bearing a targeted disruption of the *Aaas* gene. (A) Schematic representation of homologous recombination of the targeting vector, pPNT*Aaas*, with the endogenous *Aaas* gene locus: targeting vector (top), wild-type *Aaas* gene locus (middle), and mutated *Aaas* gene locus (bottom) after homologous recombination. Exons are indicated as black boxes and are numbered underneath. The orientations of the neomycin (neo) resistance marker and the herpesvirus thymidine kinase (tk) under control of the phosphoglycerate kinase promoter (PGK) are shown with arrows. The gray box marks the location of the 5′ external Southern probe. P1 to P5 indicate the primers used for detection of homologous recombinants and genotyping. (B) Southern blot analysis using DNA extracted from tail biopsies of wild-type (+/+), heterozygous (+/−), and mutant (−/−) mice. A 447-bp fragment was used as a probe, which detects an 8.5-kb wild-type and a 6.4-kb mutant hybridizable BglII fragment. (C) Northern blot analysis. Fifteen micrograms of total testes RNA from wild-type (+/+), heterozygous (+/−), and mutant (−/−) mice was separated on an agarose gel, blotted, and hybridized with an *Aaas* cDNA fragment from exons 1 and 2. After stripping, the filter was reprobed with β-actin cDNA. (D) Western blot analysis of *Aaas* expression in testes homogenates derived from wild-type (+/+) and mutant (−/−) animals. The 60-kDa ALADIN protein was detected with an antibody directed against the C terminus of ALADIN. After stripping, the membrane was reprobed with an anti-β-actin monoclonal antibody. (E) Detection of homologous recombinants in ES cells was performed by PCR assay with primers P1 and P2. Only in the case of a successful recombination was a 2.2-kb PCR product detectable. (F) PCR analysis of mouse tail DNA for genotyping of littermates with multiplex PCR using three primers (P3 to P5). The 470-bp product indicates the wild-type allele and the 730-bp product the mutant allele.

bination (Fig. 1A). The desired mutation was identified by Southern blot analysis (Fig. 1B) and confirmed by Northern blotting (Fig. 1C). Synthesis of the C-terminal 462 amino acids of ALADIN that are encoded by exons 3 to 16 were excluded by 5′ RACE and sequencing of the cDNA product. The in-frame amino acid sequence contains a stop codon immediately upstream of exon 3. Absence of the ALADIN protein was shown by Western blot analysis using a rabbit anti-ALADIN polyclonal antibody that specifically recognizes a 17-amino-acid peptide of the C terminus of ALADIN (Fig. 1D). Furthermore, PCR with different primer combinations using ES cells and mouse tail DNA was employed to confirm inactivation of the *Aaas* gene (Fig. 1E and F). Thus, the established mouse strain, designated *Aaas*$^{-/-}$, is an ALADIN null mutant.

**Characterization of *Aaas*$^{-/-}$ mice. (i) General observations.** Interbreeding of *Aaas*$^{+/-}$ mice produced litters with nearly the expected Mendelian ratio of *Aaas*$^{+/+}$, *Aaas*$^{+/-}$, and *Aaas*$^{-/-}$ mice (1:2:1). However, breeding of female *Aaas*$^{-/-}$ mice with male *Aaas*$^{+/-}$ or *Aaas*$^{-/-}$ mice did not produce any pregnancies over a period of at least 2 months, indicating that the female knockout mice are infertile. As shown below, ovaries from 6-months-old *Aaas*$^{-/-}$ mice appeared histologically normal and were capable of producing mature eggs (see Fig. 4C). In contrast, male *Aaas*$^{-/-}$ mice are able to impregnate wild-

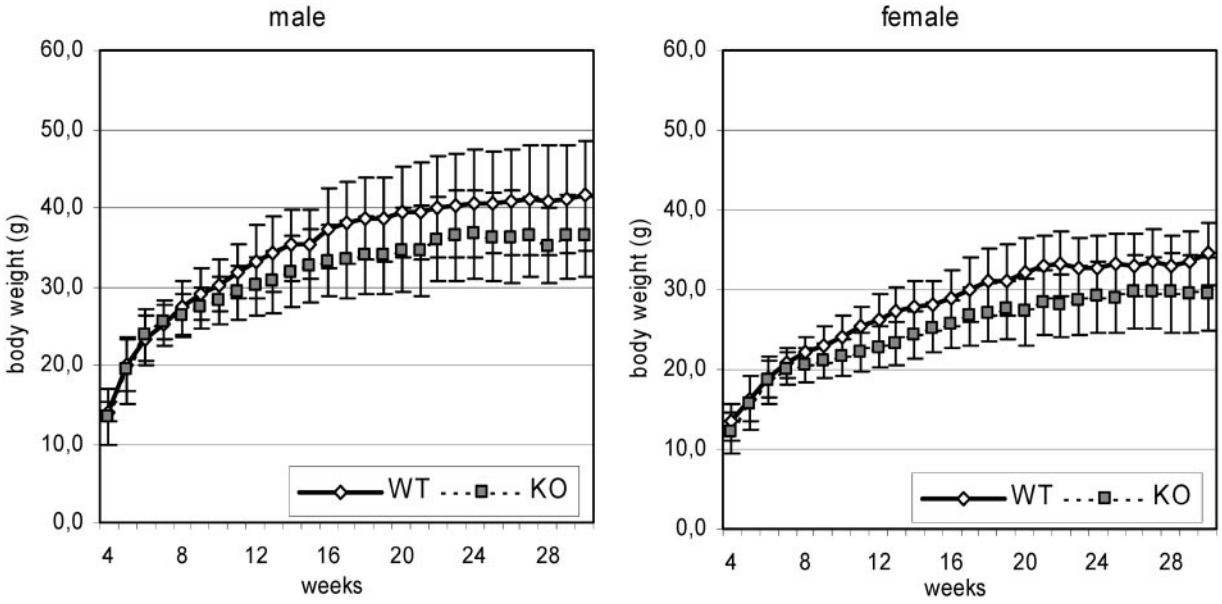


FIG. 2. Weekly measured body weight of mice at ages 4 to 30 weeks. Solid lines indicate weights of wild-type (WT) mice; dotted lines depict weights of *Aaas*$^{-/-}$ mice. Square and diamonds indicate means; error bars show ±1 standard deviation. KO, knockout.

type and *Aaas*$^{+/-}$ females. Externally, ALADIN-deficient mice were indistinguishable from their wild-type and heterozygote littermates. However, we observed a lower body weight for *Aaas*$^{-/-}$ mice than for wild-type mice. This was significant in males from the age of 10 weeks onward (except weeks 15, 22, 23, 24, and 26) and in female mice from the age of 8 weeks onward (except weeks 17 and 26) (Fig. 2). The *Aaas*$^{-/-}$ mice developed normally and did not succumb to any unusual pathological conditions. The oldest *Aaas*$^{-/-}$ mice reached an age of 2.9 (male) and 2.7 (female) years. Both wild-type and *Aaas*$^{-/-}$ mice showed normal behavior in the viewing jar and arena. Hence, no significant differences were observed in body position, spontaneous activity, defecation, or urination (viewing jar) or in transfer arousal, tail elevation, or gait (arena) (data not shown). *Aaas*$^{-/-}$ mice show the same results as wild-type mice in eye blink reflex, ear twitch reflex, visual placing reflex, whisker-orienting reflex, acoustic startle reflexes, and plantar snatch reflex (data not shown).

**(ii) Behavior.** According to the reported involvement of the central and peripheral nervous systems in human patients with *AAAS* mutations, various parameters concerning neurological reflexes, motor development, and locomotor activity were examined. The open field test is used to assess locomotor activity and anxiety-related responses. *Aaas* knockout mice were slightly less active in the open field than were the wild-type mice. The *Aaas*$^{-/-}$ mice showed a trend to spend more time resting and less time moving, they covered less distance, and they showed a lower number of circular movements than wild-type controls. This finding was significant ($P < 0.05$) in female mice at the age of 30 weeks (Fig. 3A to C). In the light-dark exploration test, there were no significant differences between genotypes for the number of light-dark transitions and percent time spent in the light versus dark compartments. However, 10- and 20-week-old male *Aaas*$^{-/-}$ mice took more time to start the first light-dark change than did age-matched wild-type mice, indicating slightly diminished exploration behavior in the male knockout mice ($P = 0.086$; data not shown).

**(iii) Motor function tests.** The Rotarod test is used to study motor coordination and skill learning. Significant differences were observed between male mice at the age of 10 weeks ($P < 0.05$), in that *Aaas*$^{-/-}$ mice were not able to remain on the rotating roller as long as their wild-type littermates (Fig. 3D). In view of the low numbers of mice that could be recruited for the Rotarod test in this age group, the importance of this result should not be overestimated, as in all other groups we were unable to detect any significant differences (Fig. 3E and F). Surprisingly, female *Aaas*$^{-/-}$ mice at an age of 20 weeks were on average able to run on the Rotarod for a longer time than the age-matched control mice (Fig. 3E).

The wire hang task, the ability to hang upside down from a wire screen, measures neuromuscular function, grip strength, and motivation. Knockout and wild-type mice fell off the screen without any significant time difference (Fig. 3G), suggesting that the *Aaas* null mutation did not result in major abnormalities in muscle strength. However, 30-week-old female *Aaas*$^{-/-}$ mice changed quadrants significantly less frequently than age-matched female wild-type mice ($P < 0.05$) (Fig. 3H), indicating diminished exploratory behavior. Furthermore, the spontaneous climbing activity of male *Aaas*$^{-/-}$ mice at the age of 30 weeks was significantly lower than that of age-matched wild-type males (Fig. 3I). In all other groups, climbing activity evaluated over 5 min did not vary significantly between wild-type and *Aaas*$^{-/-}$ mice.

**(iv) Histological and ultrastructural analysis.** Comparison of tissue sections from wild-type and *Aaas*$^{-/-}$ mice was performed on two pairs of male and female animals, respectively. In general, light microscopic examination using routine staining techniques showed no gross abnormalities in any organ systems when *Aaas*$^{-/-}$ mice were compared with their wild-type littermates. In particular, the histologies of adrenal gland,

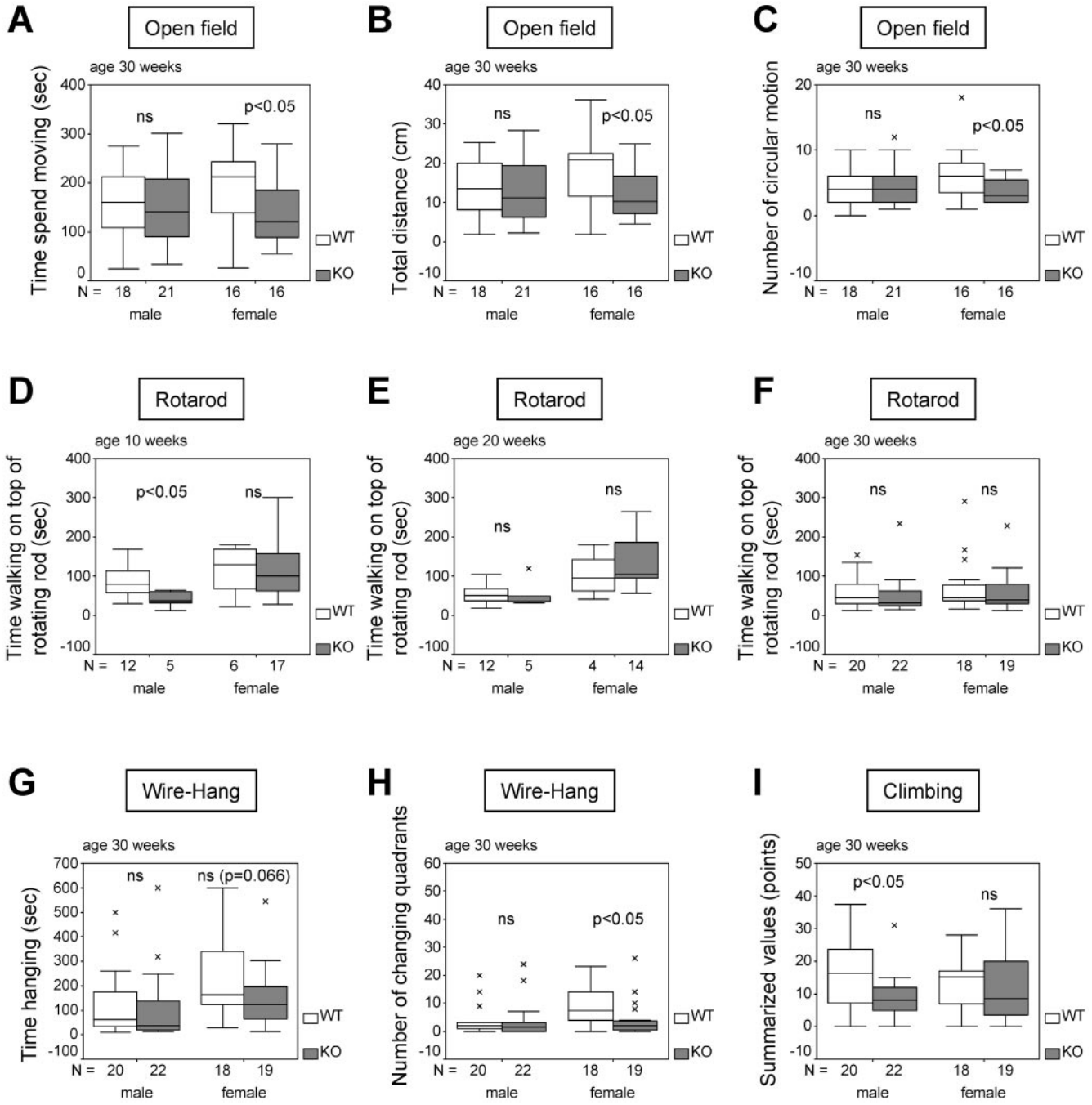


FIG. 3. Motor abilities of *Aaas*$^{+/+}$ and *Aaas*$^{-/-}$ mice. (A to C) Open field behavior. (D to F) Rotarod test. (G and H) Wire hang task. (I) Spontaneous climbing activity. Boxes, medial 50%; upper and lower lines, maximum and minimum values, respectively; black bars, medians; ×, outliers. WT, wild type; KO, knockout.

esophagus, ovary, pituitary gland, testes, and peripheral nerve did not show any differences between wild-type and ALADIN-deficient mice (Fig. 4A to F). To analyze whether the knockout of ALADIN leads to morphological changes within the cell, two types of electron microscopy experiments were performed. First, we investigated kidney and liver tissues after a classical chemical perfusion fixation of mice. With special attention paid to the nuclear pores, no morphological changes between wild-type and knockout mice tissue could be observed (Fig. 5C and D). In a second approach, we used cultured embryonic fibroblasts that were fixed by high-pressure freezing. This method preserves the ultrastructure in a more natural state and shows different features than chemical fixation. Using this method, we also did not observe any changes in NPC structure between wild-type and knockout cells (Fig. 5A and B).

**(v) Hormonal analysis.** Hormonal analyses revealed no significant differences between wild-type and *Aaas*$^{-/-}$ mice in plasma ACTH levels and serum corticosterone concentrations

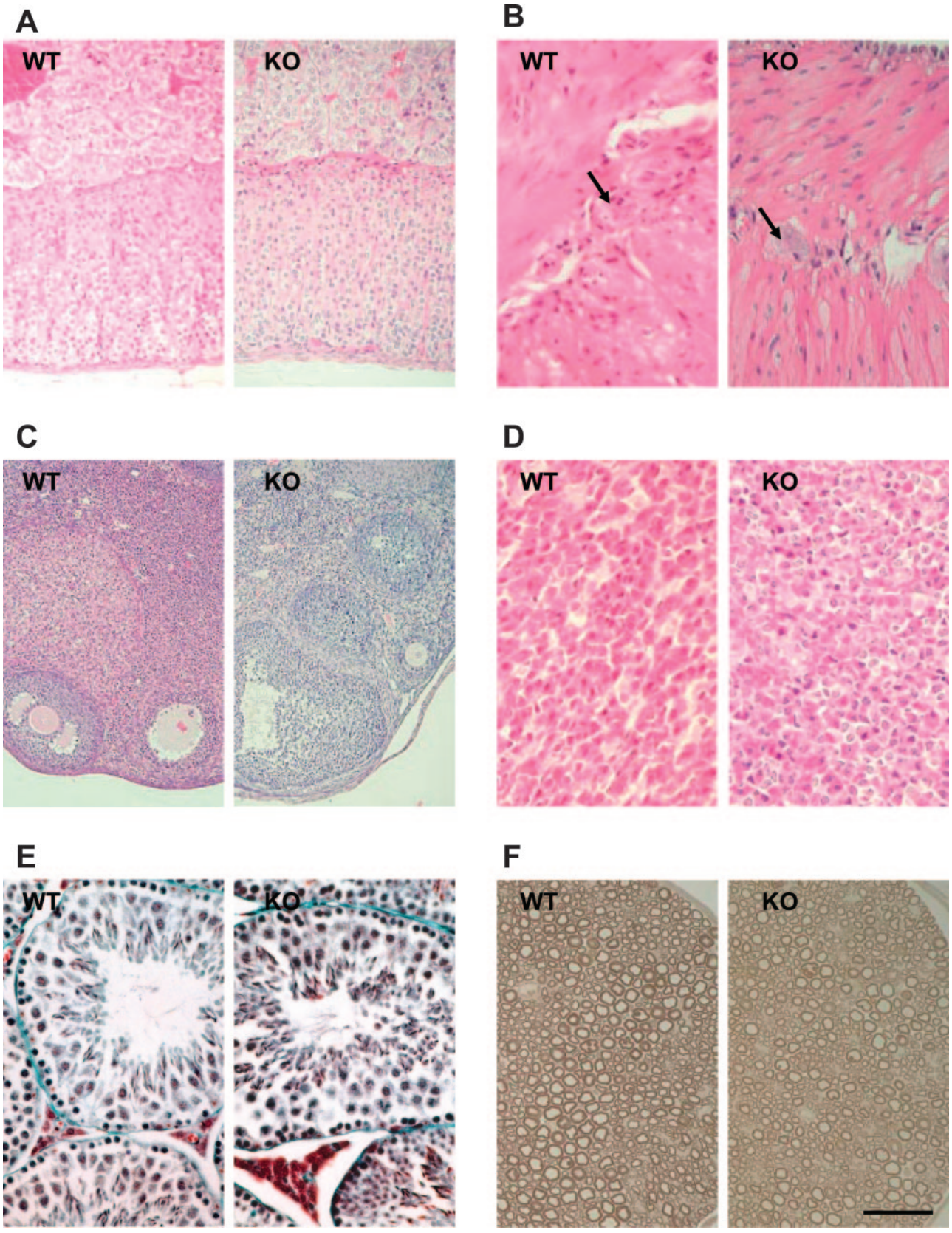


FIG. 4. Histological analysis of *Aaas*$^{+/+}$ (WT) and *Aaas*$^{-/-}$ (KO) tissue sections. (A) Adrenal gland. (B) Esophagus. Arrows indicate ganglion cells. (C) Ovary. (D) Anterior pituitary gland. (E) Testis. (F) Peripheral nerve. Tissues in panels A to D were stained with hematoxylin-eosin, tissues in panel E were stained with Goldner, and tissues in panel F were stained with *p*-phenylenediamine. Scale bar: 50 μm (B, D, E, and F), 100 μm (A), 200 μm (C).

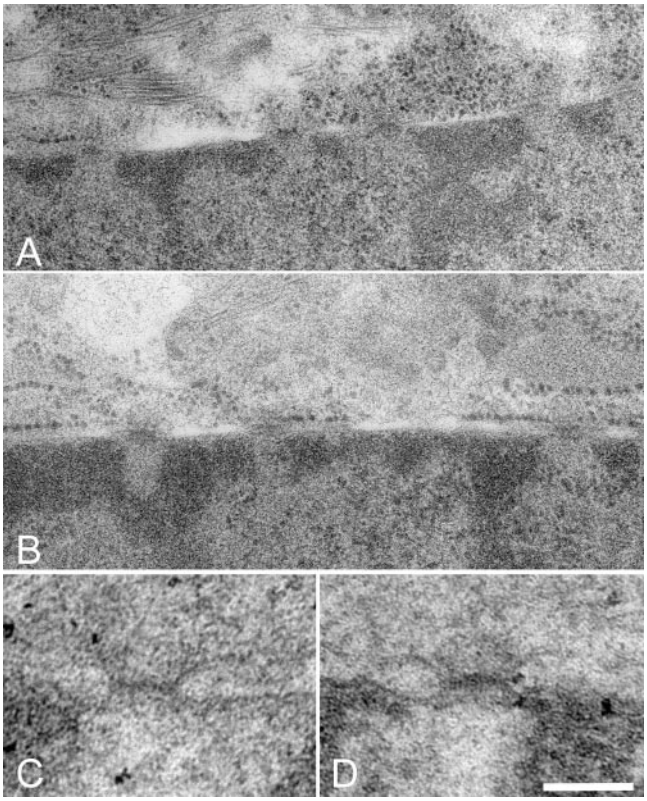


FIG. 5. Electron micrographs of nuclear pore regions of high-pressure frozen embryonic fibroblasts (A and B) and of perfusion-fixed kidney (C and D). No differences can be observed between wild-type (A and C) and *Aaas*$^{-/-}$ (B and D) cells. Scale bar: 300 nm (A and B) or 100 nm (C and D).

(Fig. 6), suggesting that the *Aaas* null mutation does not result in a disturbance of adrenocortical function in mice.

**Expression of other WD-repeat proteins from NPC.** The absence of clear phenotypic differences between wild-type and *Aaas*$^{-/-}$ mice raised the question of whether the other four WD-repeat-containing nucleoporins (Nup37, Nup43, Sec13L, RAE1) (5) might be upregulated to compensate for the lack of ALADIN protein. Northern blot analysis showed equal expression levels in wild-type, *Aaas*$^{+/-}$, and *Aaas*$^{-/-}$ mice of all four WD-repeat nucleoporins (data not shown).

## DISCUSSION

The triple A syndrome has been associated with a large number of mutations in the human *AAAS* gene, which encodes the protein ALADIN. Still, the molecular mechanisms that link ACTH-resistant adrenal failure, achalasia of the esophageal cardia, alacrima, and progressive neurological impairment remain unclear. ALADIN is a unique WD-repeat-containing component of the NPC of unknown function. We have generated ALADIN-deficient mice through standard homologous recombination within the *Aaas* gene. No ALADIN transcript or protein is detected in these animals. Surprisingly, mice deficient in ALADIN exhibit only mildly abnormal behavior and few neurological deficits. Although mutant males and heterozygous females are fertile, *Aaas*$^{-/-}$ females are sterile. Our analysis of ovaries in histological sections did not show any differences between wild-type and ALADIN-deficient mice. Follicular development and ovulation appeared to be normal, and we were not able to identify any obvious cause of infertility. However, we cannot exclude the possibility that ALADIN exhibits as yet unknown effects on the meiosis and maturation process of oocytes. We observed a notable difference between the body weights of wild-type and *Aaas*$^{-/-}$ mice; in nearly all age groups, the weight of *Aaas*$^{-/-}$ mice was significantly lower than that of wild-type mice. The cause of the differences in body weight remains unclear, as we did not find any clinical or histological signs for achalasia-like symptoms in *Aaas*$^{-/-}$ mice. Histologically, the number, size, and appearance of the myenteric ganglion cells of the lower esophagus were indistinguishable between wild-type and *Aaas*$^{-/-}$ mice. However, it cannot be excluded that ALADIN has an as yet unknown metabolic function that might be disturbed by the lack of the protein.

We demonstrate that ALADIN does not fulfill an essential function in mouse development or adult life, as the life span of

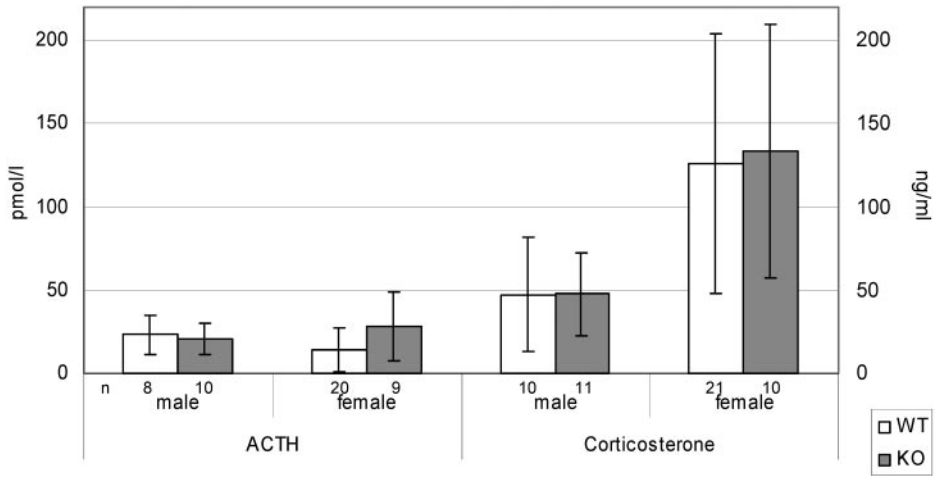


FIG. 6. ACTH concentrations (left axis) in plasma and corticosterone concentrations (right axis) in serum of wild-type (WT) and knockout (KO) mice at the age of 11 months.

*Aaas*$^{-/-}$ mice was comparable to that of wild-type mice. The finding that mice lacking ALADIN do not resemble the human triple A syndrome is important and suggests that a protein functionally replaces ALADIN within the NPCs of *Aaas*-deficient mice. We speculated that other murine nucleoporins can functionally compensate for the lack of ALADIN or that in mice the function of a putative interacting protein of ALADIN can be replaced by other proteins or biochemical pathways. A possible mechanism for functional compensation of ALADIN deficiency would be compensatory changes in expression levels of other WD-repeat proteins from NPC (Nup37, Nup43, Sec13L, RAE1). However, no differences in the RNA expression levels of Nup37, Nup43, Sec13L, or RAE1 in wild-type and *Aaas*$^{-/-}$ mice were detected. As there are no antibodies available for these proteins, the result could not be evaluated on the protein level. Experiments in which specific nucleoporins have been depleted or inactivated one by one have led to a more detailed picture of the sequence of molecular interactions that result in assembly of the vertebrate NPC (7). The disruption of the nucleoplasmically oriented Nup98 protein by using gene targeting is lethal, impairs mouse gastrulation, and triggers dramatic changes in nucleoporin stoichiometry at the cytoplasmic face of the NPC. Hence, it causes distinct protein import pathways to operate with reduced efficiency (26). In contrast to this severe phenotype, the biochemical depletion of the cytoplasmically oriented nucleoporins CAN/Nup214 and Nup358/RanBP2 from *Xenopus laevis* oocytes showed only minor (if not any) reduction in nuclear localization sequence-mediated import and no change in M9-mediated import, and in vitro-formed nuclei were normal in DNA replication (23). However, the function of single nucleoporins seems to be species specific, as the depletion of Nup214 in mice results in embryonic death and cell cycle arrest (22). Immunohistochemical investigations suggested that ALADIN resides on the cytoplasmic rather than the nuclear face (6). In contrast to Nup214, however, the elimination of ALADIN does not result in a discernible phenotype. Although we failed to detect any compensatory upregulation of the other NUP WD-repeat proteins, the lack of ALADIN in the knockout mice might be compensated for by an as yet unidentified homologue of ALADIN. It is also interesting to speculate that an unrelated protein may functionally replace ALADIN within the NPC. Such a mechanism has recently been described in knockout mice for Olp/claudin-11 and Ppl, which both represent proteins involved in central nervous system myelin formation. When either of these genes was knocked out in mice, the expression of the other protein was increased, resulting in only a mild neurological phenotype with normal-appearing myelin. However, in double-knockout mice (*Osp*/*claudin-11* and *Plp*), a severe neurological deficit, with markedly abnormal myelin compaction and small axon diameters, was observed (2).

Although we hypothesize that in *Aaas*$^{-/-}$ mice there is a protein functionally replacing ALADIN within the NPC, we cannot rule out the possibility that ALADIN is not required for a functional NPC in mice. Similar to human ALADIN-deficient fibroblasts (6), ALADIN-deficient murine cells do not show any obvious morphological defects of the NPC and nuclear envelope by electron microscopy. In humans, it is possible that ALADIN has a role in nucleocytoplasmic transport either directly, by forming transport receptor-cargo complexes at NPCs, or by mediating the assembly of macromolecular complexes or subcomplexes at the NPC (6). However, the interaction partners and potential ligands might differ between humans and mice in such a way that the overall effect of the missing ALADIN is diminished or even abolished in *Aaas*-deficient mice.

The observed weak biological effects of ALADIN deficiency in mice are unexpected. Adult animals appeared unaffected by neurological symptoms up to an age of at least 7.5 months. It could be hypothesized that the complete lack of ALADIN in mice is less harmful than the existence of a mutant, perhaps misfolded ALADIN protein. This hypothesis can be proven by generating mouse mutants that carry specified point mutations in the *Aaas* gene that have been associated with triple A syndrome in human patients. In humans, however, a dominant negative effect of a mutant allele does not exist, as heterozygous mutation carriers do not exhibit any symptoms typical for triple A syndrome. Whether an altered gene product of ALADIN results in a more dramatic phenotype in mice is currently being experimentally addressed by knock-in approaches. Future experiments should reveal whether alterations in the primary structure of ALADIN also impair the targeting, incorporation, transport, and function of other proteins of the NPC and the nucleus.

The wide range of disease severity, the obvious lack of a genotype/phenotype relationship in human patients (13), and the absence of a drastic phenotype in *Aaas*$^{-/-}$ mice suggest that additional factors, such as environmental influences or modifier genes, contribute to the disease course to a greater extent than previously anticipated. Identification of these factors will eventually shed light on the role of ALADIN at NPCs and will provide insight into how neurodevelopment is linked to NPC function.

## ACKNOWLEDGMENTS

The technical assistance of Heike Petzold, Brigitte Georgiewa, Jana Mäntler, and Ingrid Frommelt is gratefully acknowledged. We particularly thank Monika Jähkel and Gerlinde Metz for support with behavioral phenotyping and Ursula Range for help with statistical analysis. We also thank Sandra Lacas-Gervais for help with perfusion of mice. Furthermore, we thank the personnel of the Experimental Center of the Medical Faculty of the Technical University Dresden, in particular, Thomas Bernickel, for caring for the animals.

This work was supported by grants from the Deutsche Forschungsgemeinschaft to A.H. (Hu 895/3-3, 3-4, 3-5).

## REFERENCES

1. **Allgrove, J., G. S. Clayden, D. B. Grant, and J. C. Macaulay.** 1978. Familial glucocorticoid deficiency with achalasia of the cardia and deficient tear production. Lancet **i:**1284–1286.
2. **Chow, E., J. Mottahedeh, M. Prins, W. Ridder, S. Nusinowitz, and J. M. Bronstein.** 2005. Disrupted compaction of CNS myelin in an OSP/Claudin-11 and PLP/DM20 double knockout mouse. Mol. Cell. Neurosci. **29:**405–413.
3. **Clark, A. J. L., and A. Weber.** 1998. Adrenocorticotropin insensitivity syndromes. Endocr. Rev. **19:**828–843.
4. **Crawley, J., and F. K. Goodwin.** 1980. Preliminary report of a simple animal behavior model for the anxiolytic effects of benzodiazepines. Pharmacol. Biochem. Behav. **13:**167–170.
5. **Cronshaw, J. M., A. N. Krutchinsky, W. Zhang, B. T. Chait, and M. J. Matunis.** 2002. Proteomic analysis of the mammalian nuclear pore complex. J. Cell Biol. **158:**915–927.
6. **Cronshaw, J. M., and M. J. Matunis.** 2003. The nuclear pore complex protein ALADIN is mislocalized in triple A syndrome. Proc. Natl. Acad. Sci. USA **100:**5823–5827.
7. **Fahrenkrog, B., J. Koser, and U. Aebi.** 2004. The nuclear pore complex: a jack of all trades? Trends Biochem. Sci. **29:**175–182.

8. **Hadj-Rabia, S., R. Salomon, A. Pelet, C. Penet, A. Rotschild, M. H. de Laet, B. Chaouachi, R. Hannachi, F. Bakiri, R. Brauner, J. L. Chaussain, A. Munnich, and S. Lyonnet.** 2000. Linkage disequilibrium in inbred North African families allows fine genetic and physical mapping of triple A syndrome. Eur. J. Hum. Genet. **8:**613–620.
9. **Handschug, K., S. Sperling, S. J. K. Yoon, S. Hennig, A. J. L. Clark, and A. Huebner.** 2001. Triple A syndrome is caused by mutations in *AAAS*, a new WD-repeat protein gene. Hum. Mol. Genet. **10:**283–290.
10. **Holmes, A., Q. Lit, D. L. Murphy, E. Gold, and J. N. Crawley.** 2003. Abnormal anxiety-related behavior in serotonin transporter null mutant mice: the influence of genetic background. Genes Brain Behav. **2:**365–380.
11. **Huebner, A., L. L. Elias, and A. J. Clark.** 1999. ACTH resistance syndromes. J. Pediatr. Endocrinol. Metab. **12**(Suppl. 1)**:**277–293.
12. **Huebner, A., S. J. Yoon, F. Ozkinay, C. Hilscher, H. Lee, A. J. Clark, and K. Handschug.** 2000. Triple A syndrome—clinical aspects and molecular genetics. Endocr. Res. **26:**751–759.
13. **Huebner, A., A. M. Kaindl, K. P. Knobeloch, H. Petzold, P. Mann, and K. Koehler.** 2004. The triple A syndrome is due to mutations in ALADIN, a novel member of the nuclear pore complex. Endocr. Res. **30:**891–899.
14. **Irwin, S.** 1968. Comprehensive observational assessment: Ia. A systematic, quantitative procedure for assessing the behavioral and physiologic state of the mouse. Psychopharmacologia **13:**222–257.
15. **Kuhn, R., K. Rajewsky, and W. Muller.**1991. Generation and analysis of interleukin-4 deficient mice. Science **254:**707–710.
16. **Lanes, R., L. P. Plotnick, T. E. Bynum, P. A. Lee, J. F. Casella, C. E. Fox, A. A. Kowarski, and C. J. Migeon.** 1980. Glucocorticoid and partial mineralocorticoid deficiency associated with achalasia. J. Clin. Endocrinol. Metab. **50:**268–270.
17. **McIlwain, K. L., M. Y. Merriweather, L. A. Yuva-Paylor, and R. Paylor.** 2001. The use of behavioral test batteries: effects of training history. Physiol. Behav. **73:**705–717.
18. **Schumacher, H. E., J. Oehler, and M. Jaehkel.** 1994. Individual motor activity—relationships to dopaminergic responses. Pharmacol. Biochem. Behav. **48:**839–844.
19. **Stratakis, C. A., J. P. Lin, E. Pras, O. M. Rennert, C. J. Bourdony, and W. Y. Chan.** 1997. Segregation of Allgrove (triple-A) syndrome in Puerto Rican kindreds with chromosome 12 (12q13) polymorphic markers. Proc. Assoc. Am. Physicians **109:**478–482.
20. **Tullio-Pelet, A., R. Salomon, S. Hadj-Rabia, C. Mugnier, M. H. de Laet, B. Chaouachi, F. Bakiri, P. Brottier, L. Cattolico, C. Penet, M. Begeot, D. Naville, M. Nicolino, J. L. Chaussain, J. Weissenbach, A. Munnich, and S. Lyonnet.** 2000. Mutant WD-repeat protein in triple-A syndrome. Nat. Genet. **26:**332–335.
21. **Tybulewicz, V. L., C. E. Crawford, P. K. Jackson, R. T. Bronson, and R. C. Mulligan.** 1991. Neonatal lethality and lymphopenia in mice with a homozygous disruption of the c-abl proto-oncogene. Cell **65:**1153–1163.
22. **van Deursen, J., J. Boer, L. Kasper, and G. Grosveld.** 1996. G2 arrest and impaired nucleocytoplasmic transport in mouse embryos lacking the proto-oncogene CAN/Nup214. EMBO J. **15:**5574–5583.
23. **Walther, T. C., H. S. Pickersgill, V. C. Cordes, M. W. Goldberg, T. D. Allen, I. W. Mattaj, and M. Fornerod.** 2002. The cytoplasmic filaments of the nuclear pore complex are dispensable for selective nuclear protein import. J. Cell Biol. **158:**63–77.
24. **Watzman, N., and H. Berry III.** 1968. Drug effects on motor coordination. Psychopharmacologia **12:**414–423.
25. **Weber, A., T. F. Wienker, M. Jung, D. Easton, H. J. Dean, C. Heinrichs, A. Reis, and A. J. Clark.** 1996. Linkage of the gene for the triple A syndrome to chromosome 12q13 near the type II keratin gene cluster. Hum. Mol. Genet. **5:**2061–2066.
26. **Wu, X., L. H. Kasper, R. T. Mantcheva, G. T. Mantchev, M. J. Springett, and J. M. van Deursen.** 2001. Disruption of the FG nucleoporin NUP98 causes selective changes in nuclear pore complex stoichiometry and function. Proc. Natl. Acad. Sci. USA **98:**3191–3196.